Epigenetic downregulation of miRNA-34a and miRNA-449a induce epithelial-mesenchymal transition and acquired resistance to ceritinib

Sun Min Lim

Department of Medicine

The Graduate School, Yonsei University

Epigenetic downregulation of miRNA-34a and miRNA-449a induce epithelial-mesenchymal transition and acquired resistance to ceritinib

Directed by Professor Byoung Chul Cho

The Doctoral Dissertation
submitted to the Department of Medicine,
the Graduate School of Yonsei University
in partial fulfillment of the requirements for the degree
of Doctor of Philosophy

Sun Min Lim
December 2016

This certifies that the Doctoral Dissertation of Sun Min Lim is approved.

Thesis Supervisor : Byoung Chul Cho

Thesis Committee Member#1 : Joo-Hang Kim

Thesis Committee Member#2 : Hyo Sup Shim

Thesis Committee Member#3: Chang Geol Lee

Thesis Committee Member#4: Boyoun Park

The Graduate School
Yonsei University

December 2016

ACKNOWLEDGEMENTS

I would like to express my special appreciation and thanks to my advisor Professor Byoung Chul Cho, you have been a tremendous mentor for me. I would like to thank you for encouraging my research and for allowing me to grow up as a medical scientist. Your advice on the research as well as on my career as a medical oncologist has been priceless. I would also like to thank Professor Joo-Hang Kim, Professor Hyo Sup Shim, Professor Chang Geol Lee, Professor Boyoun Park for serving as my committee members even at hardship. I also would like to thank you for letting my defense be an enjoyable moment, and for your brilliant comments and suggestions, to make my research more valuable.

A special thanks to my family. Words cannot express how grateful I am to my mother, father, mother-in law, and father-in-law, for all of the sacrifices that you have made on my behalf. Your prayer for me was what sustained me thus far. I would also like to thank all of my colleagues at laboratory who supported me, and incented me to strive towards my goal. Last, but not least, I would like express my appreciation to my beloved husband Kyeong Joon Kim and my son Do Hyung Kim who were always my support and happiness in every moment.

<TABLE OF CONTENTS>

LIST OF FIGURES

LIST OF TABLES

ABSTRACT

Epigenetic downregulation of miRNA-34a and miRNA-449a induce epithelial-mesenchymal transition and acquired resistance to ceritinib

Sun Min Lim

Department of Medicine
The Graduate School, Yonsei University

(Directed by Professor Byoung Chul Cho)

Treatment with ALK tyrosine kinase inhibitors often elicits profound initial antitumor responses in ALK fusion-positive patients with lung adenocarcinoma. However, patients invariably develop acquired resistance to ALK inhibitors. Although the recent functional genetic studies characterized the mechanism of resistance to ALK inhibition, epigenetic mechanism of acquired resistance is poorly understood. Here we report histone H3 lysine 27 acetylation (H3K27ac) and microRNAs involved in acquired resistance to ceritinib, a second generation ALK inhibitor. Epithelial-to-mesenchymal transition with *AXL* activation was found in multiple *in vitro* and *in vivo* ALK-rearranged lung cancer models with acquired resistance to ceritinib. Genome-wide analysis identified that miR-34a and miR-449a are decreased

with loss of H3K27ac and *AXL* and mesenchymal genes are increased in the process of acquired resistance. Pharmacological inhibition of AXL or ectopic expression of miR-34a or miR-449a restored sensitivity to ceritinib in resistant cells. We also found histone deacetylase inhibitor, panobinostat, synergistically induced anti-proliferative effects with ceritinib in resistant cells. Our findings demonstrate that H3K27ac remodeling is a crucial event in ceritinib resistance and inhibition of both ALK and HDAC could prevent or overcome acquired resistance to ALK inhibitors in individuals with ALK-rearranged lung cancer.

Key words: non-small-cell lung cancer, acquired resistance, ceritinib, epigenetics

Epigenetic downregulation of miRNA-34a and miRNA-449a induce epithelial-mesenchymal transition and acquired resistance to ceritinib

Sun Min Lim

Department of Medicine
The Graduate School, Yonsei University

(Directed by Professor Byoung Chul Cho)

I. INTRODUCTION

EML4-ALK rearrangement is a distinct molecular subclassification of non-small-cell lung cancer (NSCLC).[1] It accounts for 4-8% of NSCLC and tumors with oncogenic *ALK* rearrangements are exquisitely sensitive to *ALK* blockade with tyrosine kinase inhibitors (TKIs) [2]. Compared with traditional chemotherapeutic drugs, treatment with ALK TKIs result in dramatic initial response with substantial duration. Crizotinib is the first FDA approved treatment for patients with *ALK*-positive NSCLC[3]. For 1st line treatment of crizotinib, the progression-free survival (PFS) is 10.9 months, and the overall response rate (ORR) is 74% [3]. However, *ALK*-positive tumors eventually develop acquired resistance to ALK TKIs within 1 year of treatment,

manifested by disease progression and leading to dismal prognosis. Ceritinib (LDK378) is a potent second-generation ALK inhibitor which can overcome resistance to crizotinib. The anticancer activity of ceritinib was shown in a phase I study for patients with *ALK*-positive NSCLC where the objective response rate was 58% for the 114 patients who were treated with ceritinib at doses above 400mg per day [4]. For patients previously treated with crizotinib, the response rate was 56%. Based on these findings, ceritinib has been granted FDA approval for treatment of patients with *ALK*-positive NSCLC in the second-line setting following failure or intolerance to crizotinib.

To date, two distinct mechanisms (*ALK*-dependent, *ALK*-independent) of acquired resistance to ALK TKIs have been known. A secondary mutation in kinase domain of *ALK* gene hinders the binding of ALK TKI. Unlike the situation with *EGFR* T790M mutation which is observed in approximately 50% of NSCLC tumors bearing activating mutations in the *EGFR* gene, the secondary mutations associated with *ALK* are diverse over a number of locations on the kinase domain[5]. Gatekeeper mutations such as L1196M, L1152R, C1156Y, and F1174L are frequently detected in crizotinib-resistant samples[6]. To date, up to one-third of patients who are progressing on crizotinib harbor resistant mutations. Friboulet and colleagues reported resistance mechanisms to ceritinib in a cohort of 11 patients who underwent biopsy at emergence of resistance to ceritinib [7]. None harbored the gatekeeper mutations which suggest the complexity of acquired resistance. Other

mechanisms of resistance are activated bypass signaling pathways (EGFR, KRAS, KIT, MET and IGF-1R), which allow continuous cell proliferation and survival[8-10], and epithelial to mesenchymal transition signature[11, 12].

While genomic mechanisms of acquired resistance have been identified, epigenomic mechanisms of ALK TKI resistance have not been elucidated. Epigenetic alterations accumulate in the noncoding genome throughout oncogenesis [13]. These involve DNA methylation or histone modification which can control expression of miRNAs and alter gene expressions involved in drug sensitivity. Previous studies have implicated that tumors exhibit not only genetic but also epigenetic heterogeneity within cell populations and that acquisition of epigenetic modifications may lead to drug resistance [14, 15]. In a study by Settleman *et al.,* drug-tolerant tumor cells emerged after altered chromatin state, which was reversible with histone deacetylase inhibitor[16]. MicroRNAs (miRNAs), a family of small, non-coding RNAs, function as gene expression regulators at posttranscriptional level[17]. They result in mRNA destabilization and translational repression [18, 19], and it is estimated that more than 30% of protein expression is regulated by endogenous miRNAs [20]. MiRNA expression was observed to be linked with tumor response to chemotherapies [21, 22], and their role in *ALK*-rearranged NSCLC remains to be identified. However, understanding the alterations in noncoding genome has been overlooked and research is especially lacking with regard to acquired resistance to ALK TKIs.

In this study, we attempted to investigate epigenetic mechanisms underlying acquired resistance to ALK TKI. Ultimately, we aimed to explore novel strategies to overcome resistance to second-generation ALK TKI.

Ⅱ. MATERIALS AND METHODS

1. Generation of resistant cells

To create ceritinib-resistant lines, H3122 and H2228 cells were cultured with increasing concentrations of ceritinib starting with the one-third maximum inhibitory concentration (IC_{30}). Doses were increased in a stepwise pattern when normal cell proliferation patterns resumed. Fresh drug was added every 72-96h. Resistant cells (H3122-LR and H2228-LR) that grew in 1μM ceritinib were derived after approximately 6 months of culturing in the continuous presence of drug. Real-time PCR showed that both the parental and resistant cells confirmed that the cells were derived from the same origin. Resistant cells were maintained initially as polyclonal populations under constant TKI selection.

2. Growth inhibition assay

For MTT assay, cultured cells were seeded into 96-well plates. Twenty-four hours after seeding, various concentrations of ceritinib were added to the culture. After 72hr, 50μl of MTT (5mg/ml stock solution) was added and the

plates were incubated for additional 4hr. The medium was discarded and the formazan blue, which was formed in the cells, was dissolved with 100 μl DMSO. The optical density was measured at 540 nm. Relative survival in the presence of drugs was normalized to DMSO control cells after background subtraction. For colony formation assays, cells were seeded into 6-well plates (2.5×10^4 cells per well) and treated with the agents in RMPI-1640 containing 10% FBS for 14 days. Compound treatments were replaced at least every 3 days during the assay. After 14 days, cells were fixed in 3% paraformaldehyde in phosphate buffered saline (PBS) for 10 min at room temperature and stained with 0.5% crystal violet in 20% methanol for 20 min. Images were captured using flatbed scanner, and the cells were dissolved with 20% acetic acids in 20% methanol for 30 min. Assays were performed independently at least three times.

3. Western blot analysis

Preparation of whole cell protein lysates and western blot analysis were described previously. Briefly, cells were then chilled on ice, washed twice with ice-cold PBS, and lysed in a buffer (Cell Signaling Technology, Beverly, MA, USA) containing 1 mM PMSF and 1X protease inhibitors (Sigma Aldrich). Protein concentrations were determined using a Bradford assay kit (Bio-Rad Laboratories). Equal amounts of protein in cell lysates were separated by SDS-PAGE, transferred to membranes, immunoblotted with

specific primary and secondary antibodies, and the blot was detected by SuperSignal West Pico Chemiluminescent Substrate (Thermo Fisher Scientific), according to the manufacturer's instructions.

4. Phospho-receptor tyrosine kinase assay

The Human Phospho-Kinase Array Kit (R&D Systems) was used to detect the activation of 49 different protein kinases mediating various aspects of cellular proliferation following the manufacturer's instructions. Briefly, H3122-LR cells were plated in 10-cm dishes and cultured at 37 °C for 28 h. After cell lysis, 500 μg of lysate was applied to a membrane-anchored phosphor kinase array and incubated at 4 °C for 24hrs. Membranes were exposed to chemiluminescent reagents and detected by X-ray film (AGFA).

5. Quantitative RT-PCR

Total RNA was isolated from cells using an RNeasy Mini Kit (Qiagen). The RNA was subjected to reverse transcription using the High-Capacity RNA-to-cDNA Kit (Life Technologies), according to the manufacturer's protocol. Quantitative RT-PCR (qRT-PCR) was performed using the fluorescent SYBR Green dye methodology and an ABI Prism 7000 Sequence Detection System (Life Technologies).

6. cDNA sequencing of ALK

Total RNA was isolated from cell pellets using the RNeasy mini kit (Qiagen, Germantown, MD, USA). The SuperScript III one-step RT-PCR system with platinum Taq DNA polymerase (Invitrogen, Carlsbad, CA, USA) was used to perform both cDNA synthesis and PCR amplification with gene-specific primers: EML4 E18F (aligned on EML4 exon 13, 5'-TTAGCATTCTTGGGGAATGG-3') and ALK_kinase_domain_R (5'-GCCTGTTGAGAGACCAGGAC-3'). The 1,223-bp PCR product, which includes the EML4-ALK fusion point and the entire ALK kinase domain, was sequenced in both directions by Sanger dideoxynucleotide sequencing.

7. Generation of in vivo resistant model

Human H3122 cells were injected subcutaneously into the flanks of CB17 SCID mice. Tumor-bearing mice (tumor size 200-500mm3) were treated with LDK378 (50mg/kg, 75mg/kg, 87.5mg/kg, 100mg/kg) administered daily. Tumors initially showed dose-dependent decrease in volume following LDK378 treatment and when tumors showed > 30% regrowth from maximal reduction, mice were sacrified to collect tumor tissue. All animal experiments were performed in compliance with the worldwide standard animal care condition via Institutional Animal Care and Use Committee (IACUC). The research proposal was approved by Yonsei University IACUC.

8. Microarray analysis

Total RNA was extracted using RNeasy columns (Qiagen, Valencia, USA) according to the manufacturer's protocol. RNA purity and integrity were evaluated by ND-1000 Spectrophotometer (NanoDrop), Agilent 2100 Bioanalyzer (Agilent Technologies). Total RNA was amplified and purified using TargetAmp-Nano Labeling Kit for Illumina Expression Bead Chip (EPICENTER) to yield biotinylated cRNA according to the manufacturer's instructions. Briefly, 200~500ng of total RNA was reverse-transcribed to cDNA using a T7 oligo (dT) primer. Second-strand cDNA was synthesized, in vitro transcribed, and labeled with biotin-NTP. After purification, the cRNA was quantified using the ND-1000 Spectrophotometer. 750ng of labeled cRNA samples were hybridizaed to each HumanHT-12 v4.0 Expression Beadchip for 16-18h at 58˚C, according to the manufacturer's instructions (Illumina, Inc.). Detection of array signal was carried out using Amershamfluorolink streptavidin-Cy3 (GE Healthcare Bio-Sciences) following the bead array manual. Arrays were scanned with an Illumina bead array Reader confocal scanner according to the manufacturer's instructions.

9. MBD-sequencing

MBD-seq was performed as described [23]. Methylated DNA was precipitated using the MethylMiner methylated DNA enrichment kit (Invitrogen). The purified methylated DNA fragments were ligated to a pair of adaptors for sequencing on the Illumina NextSeq500. Single-end reads (75 bp) were

aligned against the human reference genome 19 with the BWA aligner [24]. The MEDIPS R package (v. 1.18.0) was used for the analysis of MBD-seq data and DMR identification [25]. The Homer (v.4.8.2) software was used for the annotation of peaks and assessment of the distribution of methylation peaks across samples.

10. ChIP-sequencing

ChIP-sequencing was performed as described [26]. Cells were fixed using 1% formaldehyde, lysed and sonicated using a Bioruptor (Diagenode Inc.). Immunoprecipitation was performed with anti-H3K27ac (Millipore, 06-599) or anti-H3K4me1 (Abcam, ab8895). 250-400 bp genomic libraries were generated from the input and immunoprecipitated DNA and sequenced using Illumina NextSeq500 to generate 75 bp single-end reads. The sequencing reads were also aligned to the reference sequence (hg 19) using the Bowtie2 (v.2.2.2) software. Finding, estimation and annotation of ChIP-seq peaks were carried out by the Homer (v.4.8.2) platform [27].

11. RNA-sequencing

RNA-seq was performed as described [26]. The RNA sequencing library was prepared using the TruSeq RNA Sample Prep Kit (Illumina, San Diego, CA, USA) and the sequencing was performed based on Illumina NextSeq500 platform to generate 75 bp paired-end reads. The sequenced reads were

mapped to the human genome (hg19) using TopHat 2, and the gene expression levels were quantified with HTSeq-count module in the HTSeq package [28, 29]. The edgeR package was used to select differentially expressed genes from the RNA-seq count data [30]. Meanwhile, the FPKM value of each gene was floored to 1, and log2-transformed for further analysis (clustering, heatmap producing and correlation analysis).

12. Small RNA-sequencing

Small RNA libraries were constructed as described previously [31] with some modifications. Total RNA was isolated using the mirVana miRNA isolation kit (Ambion). Small RNAs (20 - 30 nt) were purified from 15% Novex TBE-Urea gel (Invitrogen) and ligated first with the 5' RNA adaptor and then with the 3' RNA adaptor provided by Illumina TruSeq small RNA sample preparation protocol. In each step, the ligated product was PAGE-gel purified. After first-strand synthesis and 11 cycles of PCR amplification, the product was PAGE-gel purified and submitted for sequencing on an Illumina NextSeq500 at LAS (Seoul, Korea; http://www.lascience.co.kr). After TruSeq small RNA adapters were eliminated among the sequenced reads by Trimommatic software (v.0.33), the remained sequence data were mapped to the human genome (hg19) using bowtie2 (v.2.2.2). Similar with the RNA-seq analysis procedure, the quantification and significance test were carried out using HTSeq and edgeR packages, respectively.

13. Data access

Microarray and sequencing data have been deposited in the NCBI Gene Expression Omnibus (GEO) under accession number GSE81261(for microarray) and GSE81487 (for sequencing data).

14. Apopercentage apoptosis assay

Apoptosis was detected using an APOPercentage TM kit (Biocolor, Belfast, NIreland) as described previously [32]. Phosphotidylserine at the outside surface of the cell membrane allows the unidirectional transport of the APOPercentage dye to the interior of the cell, where it is retained and accumulates as a red-dye in apoptotic cells, which can be observed in an inverted microscope and measured spectrometrically at 550nm. The treated cells in 24- or 96-well culture plates were stained with the APOPercentage dye for 1h. The medium was then removed and cells were washed twice with PBS. The levels of APOPercentage dye uptake were quantified by the colorimetric method according to the manufacturer's instruction.

15. Statistical analysis

Statistical analysis was performed using the GraphPad Prism software, version 5.0 (GraphPad Software). Student t-test was used for comparisons. All *P* values were two-sided, and values of $P < 0.05$ were regarded as statistically

significant.

III. RESULTS

1. Establishment of ALK TKI-resistant cells

For *in vitro* model, we established ceritinib resistant cell lines (H3122-LR and H2228-LR). H3122 and H2228 cells were cultured with ceritinib, gradually increasing the concentration to 1μmol/L. After 6 months of exposure to ceritinib, H3122 LR and H2228 LR cells were established. Their resistance to ceritinib was confirmed by the MTS cell proliferation assay (**Figure 1A**). Ceritinib could not inhibit phospho-ALK and the activation of ALK downstream signals, such as Akt and Erk, in both H3122-LR and H2228 -LR cells (**Figure 1B**). H3122-LR cells were also resistant to other ALK inhibitors, crizotinib and PF06463922, respectively (**Figure 1C**). We observed morphologic differences between the parental cells and resistant cells using a light microscope. The round shape of parental cells changed to spindle shaped, fibroblast-like shape, suggesting that epithelial-mesenchymal transition (EMT)-like changes may have occurred (**Figure 1D**).

To clarify the mechanisms of acquired resistance to ceritinib, we first performed DNA sequencing of a cDNA representing the ALK tyrosine kinase domain to see if known mutations were present. We did not find any secondary mutations affecting the ALK tyrosine kinase domain, spanning

exons 21-27. Next, to evaluate the activation of bypass pathways, we examined the phosphorylation level of receptor tyrosine kinases, using a human phospho-RTK array kit, in H3122-LR cells. Phospho-RTK array analysis showed increased phosphorylation of EGFR, HER2, HER3 and AXL in H3122-LR and H2228-LR cells, compared with parental cells (**Appendix 1**). To confirm this finding, we performed Western blotting of H3122 and H3122-LR cells. As expected, the phosphorylation level of AXL (Y702) was increased in H3122-LR cells, with concomitant increased level of total AXL (**Figure 1E**). AXL has previously been associated with EMT, and recent studies have suggested that therapeutic resistance may be associated with histological changes in NSCLC [11, 33, 34]. To confirm the induction of EMT in resistant cells, we analyzed the expression of epithelial and mesenchymal marker proteins using western blots. Compared to parental cells, E-cadherin was dramatically reduced, and N-cadherin expression was increased in both H3122-LR and H2228-LR cells (**Figure 1E**).

2. Elevated EMT signature in in vivo resistance model

For *in vivo* model, H3122 xenograft established in nude mice were treated with four doses of ceritinib (50mg/kg, 75mg/kg, 87.5mg/kg, and 100mg/kg) to derive ceritinib-resistant tumors. Xenograft tumors showed initial dose-dependent decrease in tumor volume and subsequently developed acquired resistance within 24-108 days (**Figure 1F, Table 1**). Sequencing of

ALK tyrosine kinase domain showed no previously known secondary mutations associated with resistance. Next, we conducted microarray expression profiling of xenograft tumors to see which genes were differentially regulated in the ceritinib-resistant tumors compared to control tumors (unpaired t test, $P < 0.05$). This analysis showed that 30 genes were highly expressed in ceritinib-resistant tumors and that EMT-related genes were significantly elevated in resistant tumors (**Figure 1G**).

Table 1. Treatment response to ceritinib in H3122 tumor xenografts

LDK378 dose (mg/kg)	Maximum tumor volume reduction	Time to maximum volume reduction	Median time to resistance
50	34.05%	18 days	24 days
75	62.20%	32 days	48 days
87.5	72.98%	42 days	62 days
100	74.25%	42 days	108 days

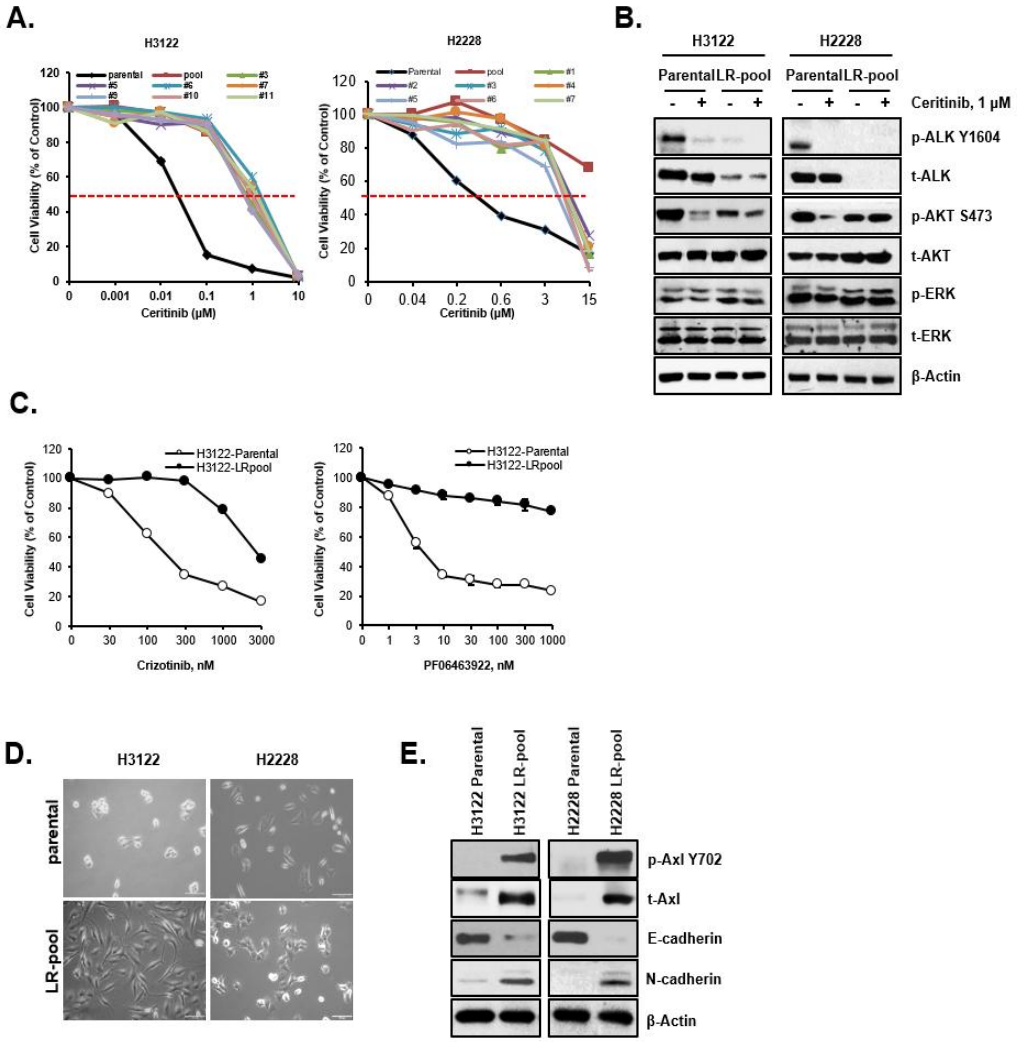

Figure 1. Ceritinib-resistant cells exhibit features of epithelial-mesenchymal transition with upregulation of AXL. (A) H3122 LR cells and H2228 LR cells were treated with ceritinib at the indicated concentrations, and viable cells were measured after 72 hours of treatment and plotted relative to parental cells. (B) H3122 parental, H3122 LR, H2228 parental, H2228 LR cells were treated with 1μM of ceritinib for 6 hours. Cell extracts were immunoblotted to detect the indicated proteins. (C) H3122 parental, H3122 LR cells were treated with crizotinib and PF-06463922 at the indicated concentrations and viable cells were measured after 72 hours of treatment. (D) H3122 parental, H3122 LR, H2228 parental, H2228 LR cells were observed using a light microscope. (E) H3122 parental, H3122 LR, H2228 parental, H2228 LR cell extracts were immunoblotted to detect the indicated proteins. (F) Mice with established H3122-derived tumors were treated with four doses of ceritinib to derive ceritinib-resistant tumors. (G) Microarray expression profiling of xenograft tumors was performed to see which genes were differentially regulated in the ceritinib-resistant tumors compared to control tumors.

3. Epigenome and transcriptome remodeling during acquired resistance to ceritinib

To investigate the epigenetic mechanisms of AXL activation and EMT induction during resistance to ceritinib, we performed methylated DNA binding domain sequencing (MBD-seq) for DNA methylation and chromatin immunoprecipitation-sequencing (ChIP-seq) for histone modifications associated with enhancers (H3K4me1 and H3K27ac) of H3122 and H3122 LR cells. MBD-seq showed similar level of average DNA methylation between H3122 and H3122 LR cells (**Figure 2A**). Among enhancer signals, average level of H3K4me1 was stable, but H3K27ac, the active enhancer signal [35], showed up to 22% decrease at the center in H3122 LR cells. A total of 52,468 H3K27ac peaks were found in H3122 cells and 11,782 peaks (22.4%) were decreased in H3122 LR cells (**Figure 2B**), suggesting loss of enhancer activity during acquired resistance to ceritinib. The regions with loss of H3K27ac were associated with protein coding genes (75%), non-coding RNAs (18%), and microRNAs (5%) within 10 kb (**Figure 2C**).

To examine the transcriptome changes in H3122 LR cells, we performed RNA sequencing (RNA-seq) in parental and LR cells and identified 802 up-regulated and 970 down-regulated genes, respectively (fold change > 2) (**Figure 2D**). Cell adhesion related genes (e.g., *N-Cadherin*, *LAMA3*, and *COL5A1*) were enriched in up-regulated genes (enrichment score 6.02), whereas apoptosis related genes (e.g., *IGFBP3*, *TNFRSF10A*, and *PDCD2*) were enriched in down-regulated genes (enrichment score 3.76). In addition to

the increased mRNA level of *AXL* (11-fold up), *GAS6*, the AXL ligand, was also increased (21-fold up). Among the down-regulated genes, 541 genes showed loss of H3K27ac. Gene ontology analysis showed that these genes are involved in regulation of phosphorylation, cell proliferation, receptor protein tyrosine kinase signaling, and apoptosis (**Figure 2E**). Among these genes, we found decreased expression of the MAPK phosphatase, *DUSP6* (25-fold down), which was previously implicated in RAS-MAPK signaling dependent-resistance to ALK inhibitors [36]. Another top down-regulated gene was the Rho GTPase, *RND1* (9-fold down), which is known to suppress EMT by retaining Ras-MAPK signaling [37].

To examine changes in the miRNA expression in H3122 LR cells, we performed small RNA-seq and identified 265 up-regulated and 188 down-regulated miRNAs. miR-221 and miR-222, which promote EMT [38] and tumorigenicity by targeting *PTEN* and *TIMP3* tumor suppressors [39], were increased in H3122 LR cells. We noted decreased expression of miR-34a which regulates *AXL* expression and promotes EMT [40], and decreased expression of miR-449 which contains similar sequences and secondary structures as the miR-34 family (**Figure 2F**) [41]. In addition, decreased H3K27ac levels of miR-34a were noted in upstream regions of H3122 LR cells.

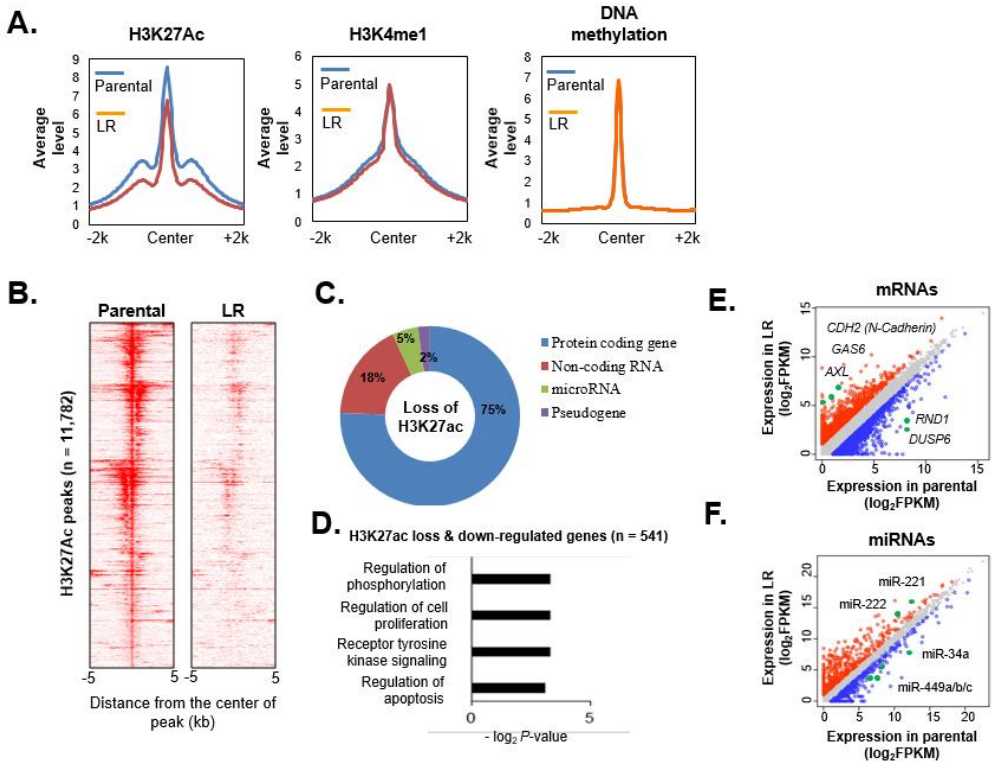

Figure 2. Dynamic changes of H3K27ac signal and transcriptome profiles in ceritinib resistant cells. (A) Plot of the average H3K27ac level, methylation level and H3K4me1 level at all peaks of parental or LR cells. (B) Heat maps of H3K27ac in parental and LR cells. 11,782 regions which showed decreased H3K27ac level in LR are selected and ranked by the difference between parental and LR. Each row represents one peak that is centered at the midpoint with a 5-kb flanking sequence. (C) Pie chart distribution of loss of H3K27ac region associated gene types. (D) Gene ontology analysis for the down-regulated genes with decreased H3K27ac levels in LR. (E) Scatter plot of mRNA expression of LR cells compared with

parental cells. Red dots indicate a >2-fold increase, and blue dots indicate a > 2-fold decrease. Positions of the indicated genes are marked by green. (F) Scatter plot of miRNA expression of LR cells compared with parental cells. Red dots indicate a >2-fold increase, and blue dots indicate a > 2-fold decrease. Positions of the indicated miRNAs are marked by green.

4. Involvement of miR-34a and miR-449 in AXL-dependent EMT gene expression

We examined whether upregulation of AXL is necessary for EMT-related changes in LR cells. When AXL inhibitor, foretinib, was treated in H3122 LR and H2228 LR cells, inhibition of p-AXL along with upregulation of E-cadherin and downregulation of N-cadherin were observed (**Figure 3A**). These data suggest that AXL activation is necessary for the acquisition of EMT phenotype in LR cells.

We observed that relative expression of miR-34a and miR-449 were significantly lower in both H3122 and H2228 LR cells, compared to parental cells. We next asked whether forced expression of miR-34a and miR-449a regulate *AXL*-dependent EMT gene expression. We first confirmed the activity of mimics and inhibitors of miR-34a and miR-449a. Treatment of miR-34a and miR-449a mimics in H3122 LR cells induced significant increase in their expression, and treatment of inhibitors of miR-34a and miR-449a induced significant decrease in their expression (**Appendix 2**). When mimics of miR-34a and miR-449a were treated in H3122 LR cells, p-AXL and N-cadherin were downregulated with upregulation of E-cadherin. When inhibitors of miR-34a and miR-449a were treated in parental cells, p-AXL and N-cadherin were upregulated with downregulation of E-cadherin (**Figure 3B**). These data suggest that miR-34a and miR-449a negatively regulate AXL-dependent EMT gene expression in acquired resistance to ceritinib.

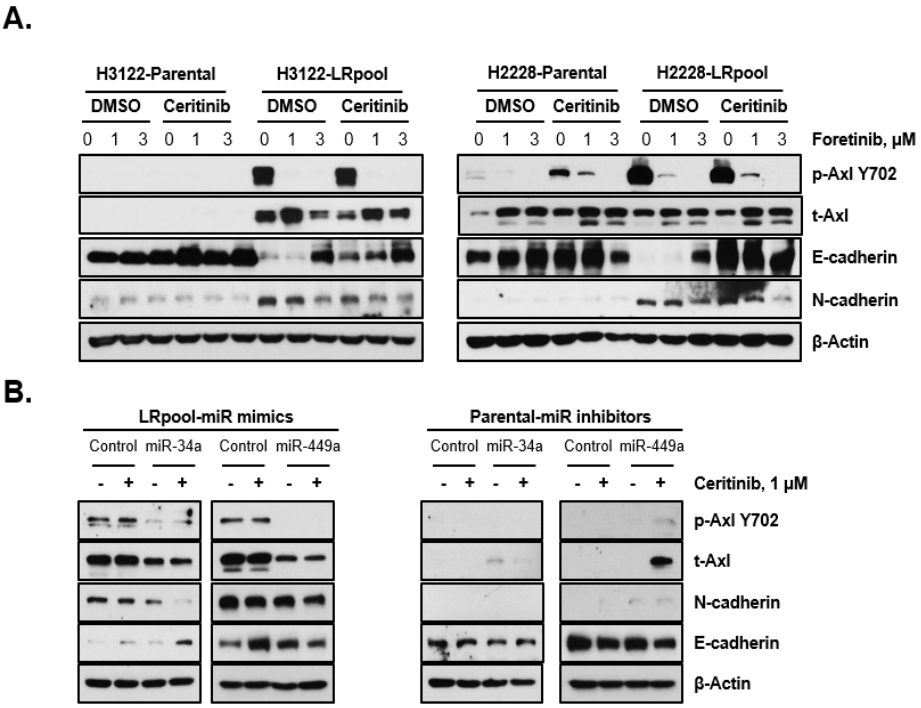

Figure 3. Involvement of miR-34a and miR-449a in *AXL*-dependent EMT gene expression (A) H3122 parental, H3122 LR, H2228 parental, H2228 LR cells were treated with foretinib at the indicated concentrations and immunoblotted to detect the indicated proteins. Inhibition of p-AXL along with upregulation of E-cadherin and downregulation of N-cadherin were observed. (B) Mimics of miR-34a and miR-449a were treated in H3122 LR cells, and inhibitors of miR-34a and miR-449a were treated in parental cells. Ceritinib 1μM was treated and indicated proteins involving AXL and EMT gene expression were immunoblotted. When mimics of miR-34a and miR-449a were treated in LR cells, p-AXL and N-cadherin were

downregulated with upregulation of E-cadherin. When inhibitors of miR-34a and miR-449a were treated in parental cells, p-AXL and N-cadherin were upregulated with downregulation of E-cadherin.

Our aim was then to determine whether miR-34a and miR-449a could influence ceritinib sensitivity. We investigated whether miR-449a mimics can reverse resistance in H3122 LR cells, and whether miR-449a inhibitor can confer resistance in H3122 parental cells. As expected, treatment of miR-449a mimics re-sensitized H3122-LR cells to ceritinib, and treatment of miR-449a inhibitor induced resistance to ceritinib (**Figure 4A**). Accordingly, treatment of miR-34a and miR-449a mimics in LR cells led to decreased p-AKT, and p-ERK upon ceritinib treatment. Treatment of miR-34a and miR-449a inhibitors in parental cells did not downregulate p-AKT and p-ERK upon ceritinib treatment (**Figure 4B**).

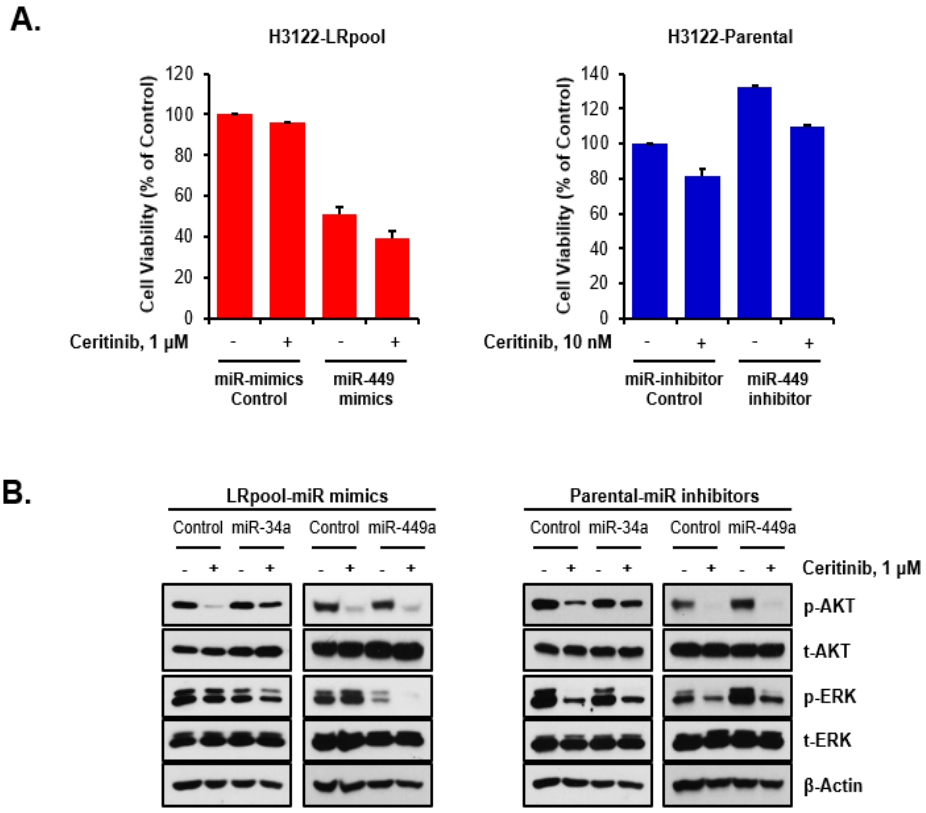

Figure 4. MiR-34a and miR-449a affect ceritinib sensitivity. (A) Treatment of miR-449a mimics re-sensitized H3122-LR cells to ceritinib, and treatment of miR-449a inhibitor induced resistance to ceritinib. (B) Treatment of miR-34a and miR-449a mimics in LR cells led to decreased p-AKT, and p-ERK upon ceritinib treatment. Treatment of miR-34a and miR-449a inhibitors in parental cells did not downregulate p-AKT and p-ERK upon ceritinib treatment.

5. Panobinostat changes H3K27ac profiles and expression of miRNAs

We next examined whether treatment of the histone deacetylase inhibitor panobinostat (LBH589) can reverse H3K27ac profiles of LR cells. We conducted RNA-seq and ChIP-seq after treatment with panobinostat. We found 22,810 regions showing increased H3K27ac level by panobinostat treatment (30nM). There was no significant difference in H3K27ac profile between combination treatment of panobinostat (30 nM) and ceritinib (10 nM) and panobinostat only (**Figure 5A**). Among the downregulated miRNAs in LR cells, 70% maintained low expression levels (e.g., miR-34a, miR-375, and miR-29b-2), while 30% showed increased expression level (e.g., miR-449, miR-192, and miR-212; **Figure 5B**). We also found increased expression of 45 miRNAs which were not decreased in LR cells (e.g., miR-2171, miR-144, and miR-184), after panobinostat treatment (**Figure 5B**). Regardless of panobinostat treatment, miR-34a maintained reduced H3K27ac signal (**Figure 5C**) and low expression level (**Figure 5D**). On the contrary, miR-449 showed increased H3K27ac signal (**Figure 5E**) and a significant increase in expression level (**Figure 5F**) with panobinostat treatment.

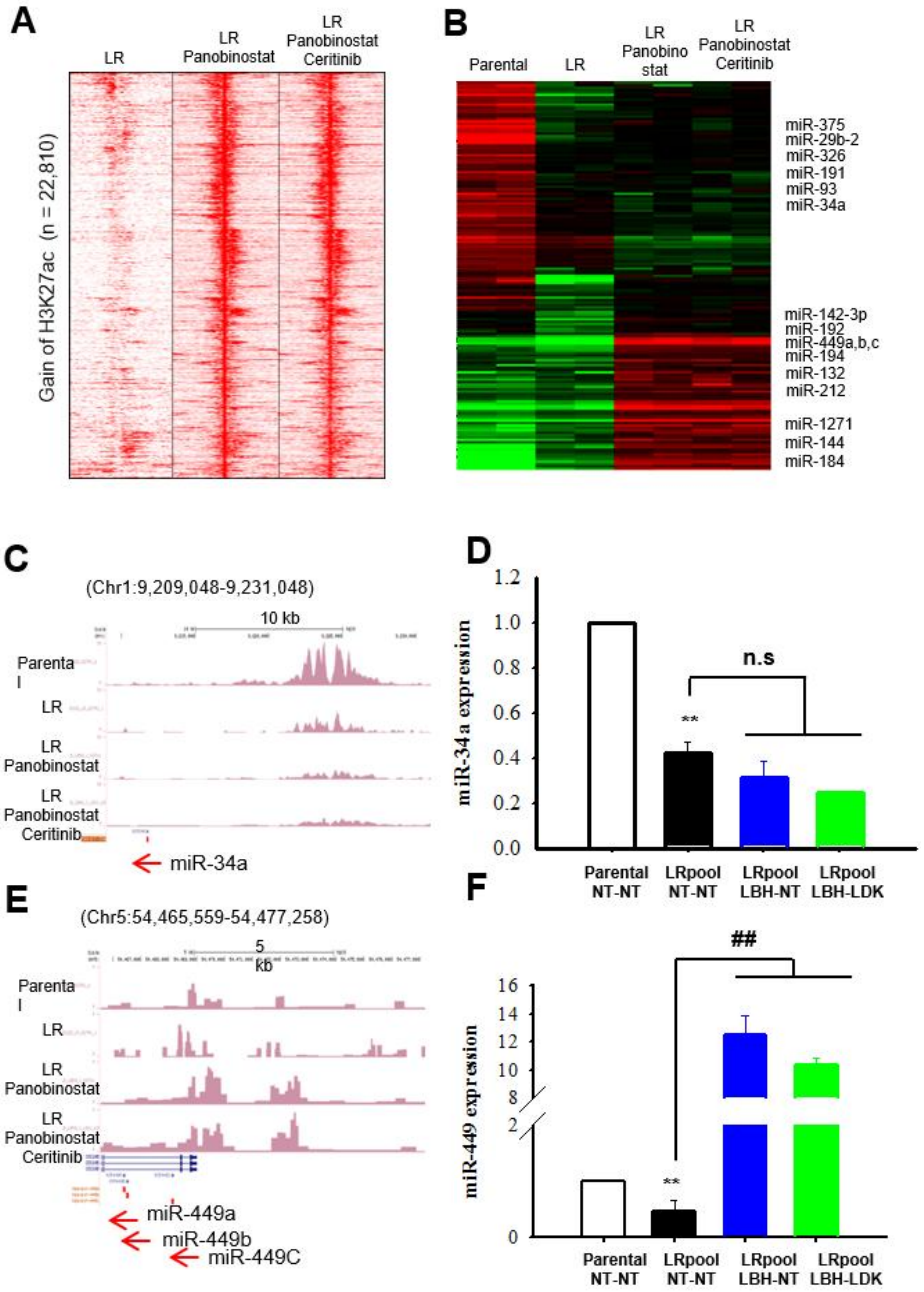

Figure 5. Panobinostat induced changes of H3K27ac signal and miRNAs expression (A) Heat maps of H3K27ac in ceritinib resistant cells with

panobinostat treatment or panobinostat and ceritinib combination. 22,810 regions which showed increased H3K27ac level in panobinostat treated cells are selected and ranked by the difference between panobinostat treated LR and LR. Each row represents one peak that is centered at the midpoint with a 5-kb flanking sequence. (B) Heat map of relative expression levels of miRNAs which were down-regulated with acquired resistance of ceritinib or up-regulated with panobinostat treatment. Green represents relatively low expression and red, relatively high expression (C) Genome browser view of H3K27ac ChIP-seq data of miR-34a in four cells (H3122 parental, H3122 LR, panobinostat treated H3122 LR, and panobinostat and ceritinib co-treated H3122 LR). (D) qRT-PCR analysis of miR-34a. (E) Genome browser view of H3K27ac ChIP-seq data of miR-449a/b/c. (F) qRT-PCR analysis of miR-449a.

6. HDAC inhibition restores sensitivity to ceritinib in acquired resistant cells

Next, we examined whether panobinostat could restore sensitivity to ceritinib. Colony formation assays revealed synergistic antitumor effects of panobinostat with ceritinib when treated in H3122- and H2228 LR cells and the efficacy was dose-dependent (**Figure 6A**). Apoptosis assay showed significant increase in apoptotic cells when H3122- and H2228 LR cells were treated with panobinostat or ceritinib plus panobinostat (**Figure 6B-C**). When apoptosis-related markers were examined by western blot, panobinostat treatment increased phosphorylation of cleaved PARP, cleaved caspase 3, and decreased phosphorylation of p21 and cyclin D1 (**Figure 6D**). Cell cycle assay of H3122- and H2228 LR cells showed that ceritinib and panobinostat treatment induced arrest of the cells at the G1 phase. (**Figure 6E**). In addition, panobinostat treatment regulated downstream effector genes of miR-34a and miR-449a, by downregulating p-AXL, t-MET, and c-MYC. Panobinostat also reversed EMT phenotype by downregulating N-cadherin and upregulating E-cadherin expression (**Figure 6F**).

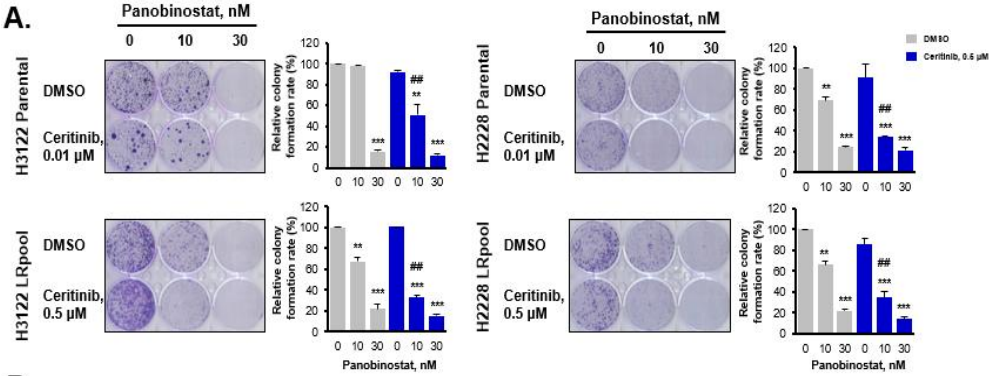

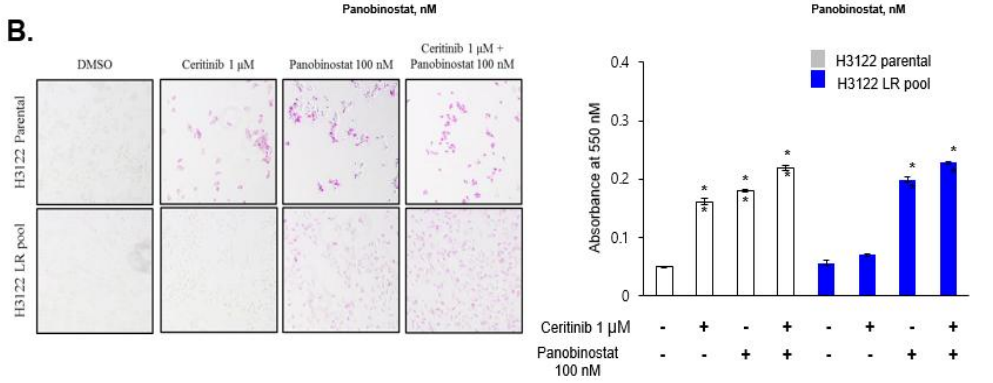

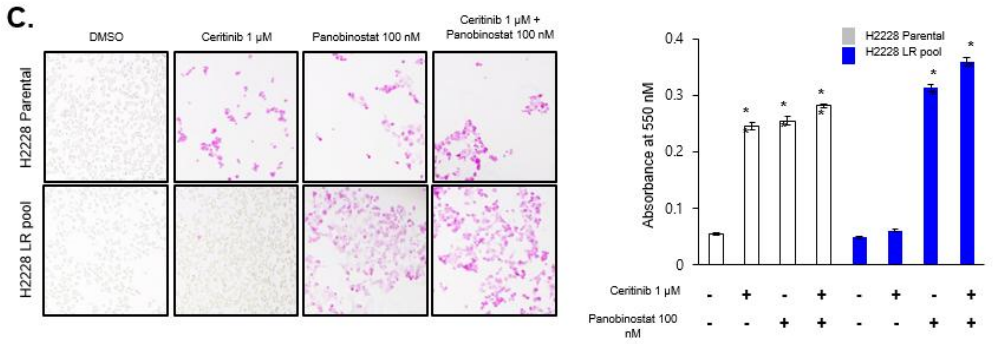

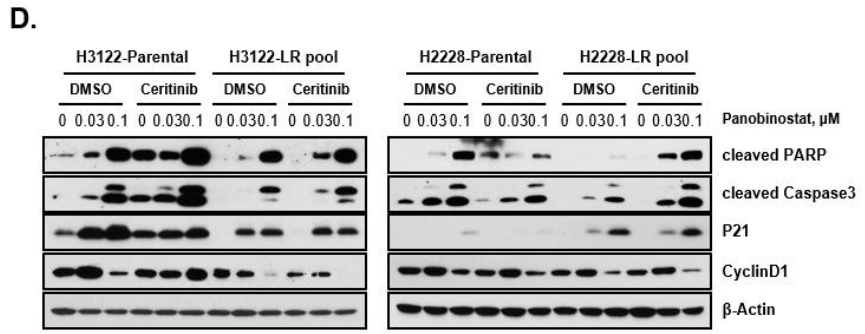

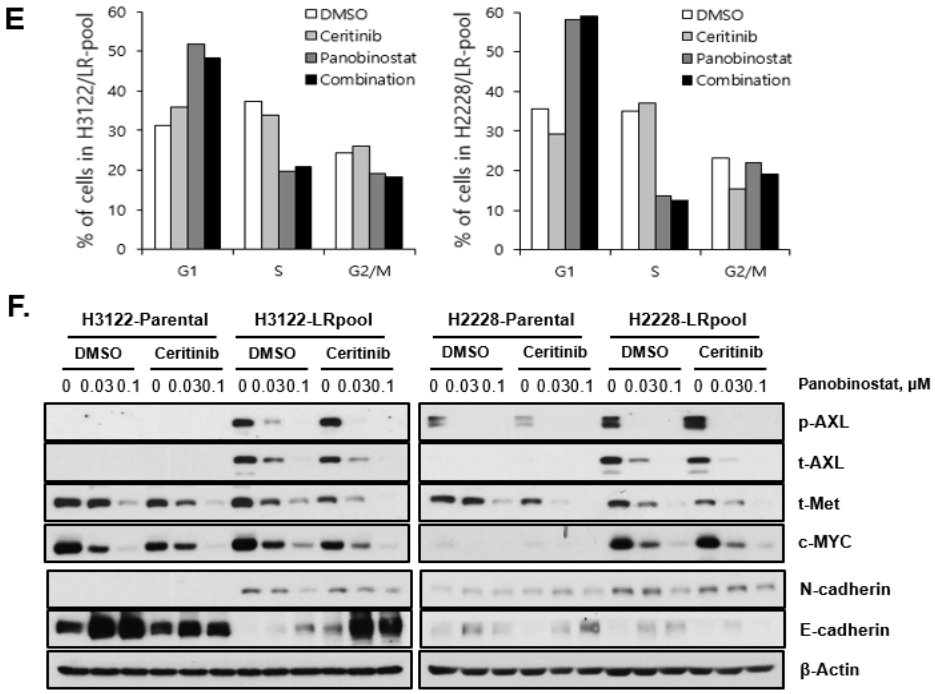

Figure 6. Synergistic anti-proliferative effects of panobinostat and ceritinib in ceritinib-acquired resistant cells (A) Colony formation assays in H3122 parental, H3122 LR, H2228 parental, H2228 LR cells showed synergistic anti-proliferative efficacy of ceritinib and panobinostat. (B) Apoptosis assay showed significant increase in apoptotic cells when H2228 LR cells were treated with ceritinib plus panobinostat (C) Apoptosis assay showed significant increase in apoptotic cells when H3122 LR cells were treated with ceritinib plus panobinostat (D) Apoptosis-related markers were examined by western blot after treatment with panobinostat. (E) Cell cycle assay showed that ceritinib and panobinostat treatment induced arrest of the

cells at the G1 phase. (F) Panobinostat treatment regulated downstream effector genes of miR-34a and miR-449a and reversed EMT phenotype by downregulating N-cadherin and upregulating E-cadherin expression.

7. Combination of HDAC inhibitor and ceritinib induces enhanced antitumor efficacy in acquired resistant xenograft models

H3122 xenograft tumors were established in nude mice, and were treated with LDK378 75mg/kg to derive ceritinib-resistant tumors. Resistant tumors were randomized to four treatment groups (vehicle, LDK378 75mg/kg, LBH 50mg, LDK378 75mg/kg and LBH 50mg/kg), each group consisting of 5 mice. Consistent with the *in vitro* findings, combination treatment with LDK378 and LBH displayed superior antitumor efficacy compared with monotherapy of LBH.

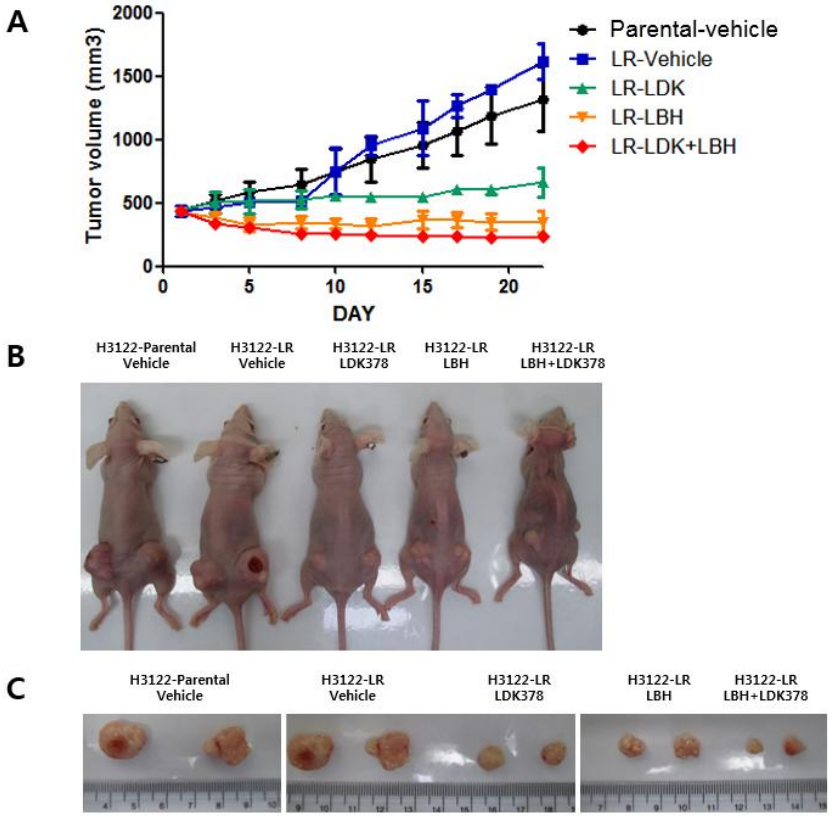

Figure 7. Enhanced activity of panobinostat in combination with ceritinib *in vivo* (A) Ceritinib-resistant tumors were treated with vehicle, LDK378 75mg/kg, LBH 50mg/kg, LDK378 75mg/kg and LBH 50mg/kg, as indicated. (B) Photographs of representative mice with tumors from each group (C) Photographs of excised tumors from each group

Ⅳ. DISCUSSION

In this study, we discovered that H3K27ac remodeling and changes in miRNA expression are crucial events in ceritinib resistance. Reduced expression of miR-34a and miR-449a with decreased H3K27ac led to upregulation of AXL and EMT related genes in ceritinib resistant cells. Moreover, treatment of HDAC inhibitor, panobinostat increased H3K27ac signal and restored sensitivity to ceritinib. (**Figure 7**). To our knowledge, this is the first study to report epigenetic regulation of acquired resistance mechanism using *in vitro*, *in vivo ALK*-positive lung cancer models.

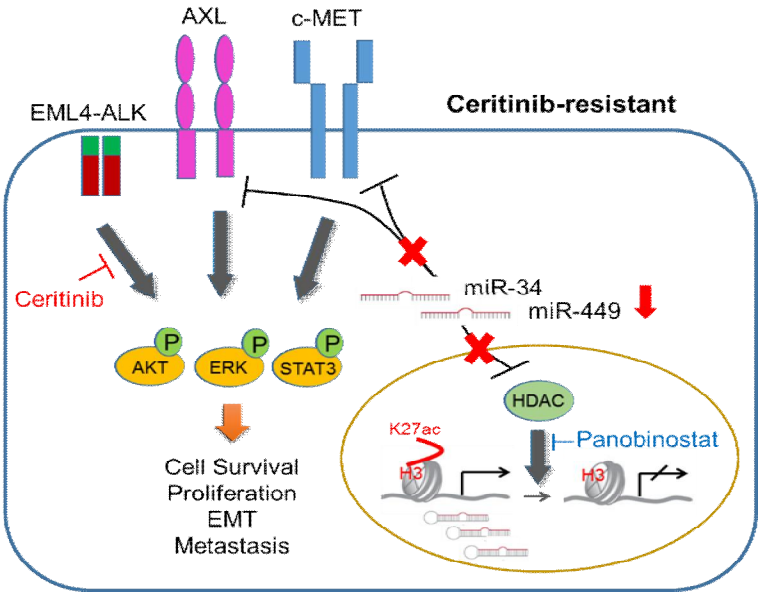

Figure 8. Schematic diagram of ceritinib resistance mechanism involving epigenetic regulation of miRNAs

Although ceritinib is the treatment of choice in crizotinib-refractory

ALK-positive NSCLC patients, most patients eventually develop resistance. While various mechanisms of resistance to crizotinib have been known, only secondary mutations in the *ALK* gene have been identified as mechanisms of acquired resistance to ceritinib[7, 42]. To date, *ALK* G1202R, F1174C/V and most recently, G1123S mutation were identified in a patient with exhibiting resistance to ceritinib. These resistant mutations can be overcome by a highly potent, third-generation ALK inhibitor, such as lorlatinib. However, resistance mechanisms other than secondary mutations are largely unknown and strategies to overcome have not been investigated.

In our study, H3122 LR and H2228 LR cells and xenograft model exhibited elevated expression of EMT-related genes. RNA sequencing of H3122 parental and H3122 LR cells showed increased mRNA expression of *AXL* and its ligand, GAS6. In addition, EMT-associated transcriptional changes involving upregulation of vimentin and downregulation of E-cadherin were observed. In addition, EMT has been previously reported as an acquired resistance mechanism of crizotinib[11, 12]. Yet, our study uncovers a distinct mechanism of acquired resistance by identifying microRNAs which regulate AXL and EMT-related gene expression.

MicroRNAs and their roles in therapy resistance have been previously studied in various cancers[43-45]. Regulation of EMT by miRNAs in ALK-positive cell line has been recently reported by Gao *et al.* that miR-200c directly targets ZEB1 and thereby increasing E-cadherin expression, which in

turn, suggests that miR-200c can prevent EMT in H2228 cells by targeting ZEB1[46] .

Since epigenetic mechanisms have crucial roles in EMT, we focused on epigenetic changes in ceritinib resistance[47]. Through ChIP-seq, we noted that H3K27ac peaks were decreased in H3122 LR cells compared to H3122 parental cells, suggesting loss of enhancer activity during acquired resistance to ceritinib. Genome-wide H3K27ac profiles showed decreased H3K27ac signals in many genomic regions in LR cells and 5% of these regions were associated with miRNAs within 10kb. Among 188 downregulated miRNAs in resistant cells, decreased H3K27ac levels of miR-34a and miR-449a were notable. Expression levels of miR-34a and miR-449a, which downregulate *AXL* expression, were also decreased[41]. MiR-34a is known to antagonize many different oncogenic processes such as apoptosis, proliferation, invasion and migration[48]. MiR-449a is a potent inducer of cell death, cell cycle arrest, and/or cell differentiation[41]. They belong to the same family and are structurally related. In our study, deacetylation of miR-34a and miR-449a led to altered expression of their target genes associated with EMT, apoptosis and cell cycle. Re-introduction of miR-34a and miR-449a sensitized H3122 LR cells to ceritinib.

Intriguingly, panobinostat treatment induced synergistic anti-proliferative effects in ceritinib-resistant cells. Panobinostat is a potent, pan-HDAC inhibitor which blocks class I, II and IV HDACs. It is currently approved for

the treatment of relapsed and refractory multiple myeloma, in which both bortezomib and immunomodulatory drugs have failed [49]. Panobinostat induced site-specific increase of H3K27ac, as represented by increased miR-449 expression. Our observations suggest that panobinostat in combination with ceritinib will overcome acquired resistance to ceritinib. Combination strategy of ceritinib and panobinostat is feasible since they do not have overlapping grade 3/4 toxicities. Ceritinib has gastrointestinal toxicities such as elevated liver enzymes and diarrhea, whereas panobinostat has hematological toxicities such as neutropenia and thrombocytopenia[50]. This provides a rationale for the development of HDAC inhibitor for clinical use of ALK-positive advanced NSCLC patients to either prevent or overcome resistance to ALK TKIs.

V. CONCLUSION

H3K27ac remodeling and changes in miRNA expression such as miR-34a and miR-449a should be considered as a novel acquired resistance mechanism associated with ceritinib, and panobinostat may be a promising option for overcoming ceritinib resistance.

REFERENCES

1. Shaw AT, Yeap BY, Mino-Kenudson M, Digumarthy SR, Costa DB, Heist RS, et al. Clinical features and outcome of patients with non-small-cell lung cancer who harbor EML4-ALK. J Clin Oncol 2009;27(26):4247-53.

2. Crystal AS, Shaw AT. New targets in advanced NSCLC: EML4-ALK. Clinical advances in hematology & oncology : H&O 2011;9(3):207-14.

3. Shaw AT, Kim DW, Nakagawa K, Seto T, Crino L, Ahn MJ, et al. Crizotinib versus chemotherapy in advanced ALK-positive lung cancer. The New England journal of medicine 2013;368(25):2385-94.

4. Shaw AT, Kim DW, Mehra R, Tan DS, Felip E, Chow LQ, et al. Ceritinib in ALK-rearranged non-small-cell lung cancer. The New England journal of medicine 2014;370(13):1189-97.

5. Doebele RC, Pilling AB, Aisner DL, Kutateladze TG, Le AT, Weickhardt AJ, et al. Mechanisms of resistance to crizotinib in patients with ALK gene rearranged non-small cell lung cancer. Clinical cancer research : an official journal of the American Association for Cancer Research 2012;18(5):1472-82.

6. Choi YL, Soda M, Yamashita Y, Ueno T, Takashima J, Nakajima T, et al. EML4-ALK mutations in lung cancer that confer resistance to ALK inhibitors. The New England journal of medicine 2010;363(18):1734-9.

7. Friboulet L, Li N, Katayama R, Lee CC, Gainor JF, Crystal AS, et al. The ALK inhibitor ceritinib overcomes crizotinib resistance in non-small cell lung cancer. Cancer discovery 2014;4(6):662-73.

8. Sasaki T, Koivunen J, Ogino A, Yanagita M, Nikiforow S, Zheng W, et al. A novel ALK secondary mutation and EGFR signaling cause resistance to ALK kinase inhibitors. Cancer research 2011;71(18):6051-60.

9. Tanizaki J, Okamoto I, Okabe T, Sakai K, Tanaka K, Hayashi H, et al. Activation of HER family signaling as a mechanism of acquired resistance to

ALK inhibitors in EML4-ALK-positive non-small cell lung cancer. Clinical cancer research : an official journal of the American Association for Cancer Research 2012;18(22):6219-26.

10. Katayama R, Shaw AT, Khan TM, Mino-Kenudson M, Solomon BJ, Halmos B, et al. Mechanisms of acquired crizotinib resistance in ALK-rearranged lung Cancers. Science translational medicine 2012;4(120):120ra17.

11. Kim HR, Kim WS, Choi YJ, Choi CM, Rho JK, Lee JC. Epithelial-mesenchymal transition leads to crizotinib resistance in H2228 lung cancer cells with EML4-ALK translocation. Molecular oncology 2013;7(6):1093-102.

12. Sang J, Acquaviva J, Friedland JC, Smith DL, Sequeira M, Zhang C, et al. Targeted inhibition of the molecular chaperone Hsp90 overcomes ALK inhibitor resistance in non-small cell lung cancer. Cancer discovery 2013;3(4):430-43.

13. Zhou S, Treloar AE, Lupien M. Emergence of the Noncoding Cancer Genome: A Target of Genetic and Epigenetic Alterations. Cancer discovery 2016;6(11):1215-29.

14. Brock A, Chang H, Huang S. Non-genetic heterogeneity--a mutation-independent driving force for the somatic evolution of tumours. Nat Rev Genet 2009;10(5):336-42.

15. Wilting RH, Dannenberg JH. Epigenetic mechanisms in tumorigenesis, tumor cell heterogeneity and drug resistance. Drug Resist Updat 2012;15(1-2):21-38.

16. Sharma SV, Lee DY, Li B, Quinlan MP, Takahashi F, Maheswaran S, et al. A chromatin-mediated reversible drug-tolerant state in cancer cell subpopulations. Cell 2010;141(1):69-80.

17. Ambros V. The functions of animal microRNAs. Nature 2004;431(7006):350-5.

18. Cheng AM, Byrom MW, Shelton J, Ford LP. Antisense inhibition of human miRNAs and indications for an involvement of miRNA in cell growth and apoptosis. Nucleic Acids Res 2005;33(4):1290-7.

19. Krol J, Loedige I, Filipowicz W. The widespread regulation of microRNA biogenesis, function and decay. Nat Rev Genet 2010;11(9):597-610.

20. Friedman RC, Farh KK, Burge CB, Bartel DP. Most mammalian mRNAs are conserved targets of microRNAs. Genome Res 2009;19(1):92-105.

21. Berman M, Mattheolabakis G, Suresh M, Amiji M. Reversing epigenetic mechanisms of drug resistance in solid tumors using targeted microRNA delivery. Expert Opin Drug Deliv 2016:1-12.

22. Bian HB, Pan X, Yang JS, Wang ZX, De W. Upregulation of microRNA-451 increases cisplatin sensitivity of non-small cell lung cancer cell line (A549). J Exp Clin Cancer Res 2011;30:20.

23. Kim M, Park YK, Kang TW, Lee SH, Rhee YH, Park JL, et al. Dynamic changes in DNA methylation and hydroxymethylation when hES cells undergo differentiation toward a neuronal lineage. Hum Mol Genet 2014;23(3):657-67.

24. Li H, Durbin R. Fast and accurate long-read alignment with Burrows-Wheeler transform. Bioinformatics 2010;26(5):589-95.

25. Lienhard M, Grimm C, Morkel M, Herwig R, Chavez L. MEDIPS: genome-wide differential coverage analysis of sequencing data derived from DNA enrichment experiments. Bioinformatics 2014;30(2):284-6.

26. Baek SJ, Kim M, Bae DH, Kim JH, Kim HJ, Han ME, et al. Integrated epigenomic analyses of enhancer as well as promoter regions in gastric cancer. Oncotarget 2016.

27. Zhang Y, Liu T, Meyer CA, Eeckhoute J, Johnson DS, Bernstein BE, et al. Model-based analysis of ChIP-Seq (MACS). Genome Biol

2008;9(9):R137.

28. Anders S, Pyl PT, Huber W. HTSeq--a Python framework to work with high-throughput sequencing data. Bioinformatics 2015;31(2):166-9.

29. Kim D, Pertea G, Trapnell C, Pimentel H, Kelley R, Salzberg SL. TopHat2: accurate alignment of transcriptomes in the presence of insertions, deletions and gene fusions. Genome Biol 2013;14(4):R36.

30. Robinson MD, McCarthy DJ, Smyth GK. edgeR: a Bioconductor package for differential expression analysis of digital gene expression data. Bioinformatics 2010;26(1):139-40.

31. Lu C, Meyers BC, Green PJ. Construction of small RNA cDNA libraries for deep sequencing. Methods 2007;43(2):110-7.

32. Keter FK, Kanyanda S, Lyantagaye SS, Darkwa J, Rees DJ, Meyer M. In vitro evaluation of dichloro-bis(pyrazole)palladium(II) and dichloro-bis(pyrazole)platinum(II) complexes as anticancer agents. Cancer chemotherapy and pharmacology 2008;63(1):127-38.

33. Debruyne DN, Bhatnagar N, Sharma B, Luther W, Moore NF, Cheung NK, et al. ALK inhibitor resistance in ALK-driven neuroblastoma is associated with AXL activation and induction of EMT. Oncogene 2015.

34. Wu F, Li J, Jang C, Wang J, Xiong J. The role of Axl in drug resistance and epithelial-to-mesenchymal transition of non-small cell lung carcinoma. Int J Clin Exp Pathol 2014;7(10):6653-61.

35. Creyghton MP, Cheng AW, Welstead GG, Kooistra T, Carey BW, Steine EJ, et al. Histone H3K27ac separates active from poised enhancers and predicts developmental state. Proceedings of the National Academy of Sciences of the United States of America 2010;107(50):21931-6.

36. Hrustanovic G, Olivas V, Pazarentzos E, Tulpule A, Asthana S, Blakely CM, et al. RAS-MAPK dependence underlies a rational polytherapy strategy in EML4-ALK-positive lung cancer. Nature medicine 2015;21(9):1038-47.

37. Okada T, Sinha S, Esposito I, Schiavon G, Lopez-Lago MA, Su W, et al. The Rho GTPase Rnd1 suppresses mammary tumorigenesis and EMT by restraining Ras-MAPK signalling. Nature cell biology 2015;17(1):81-94.

38. Garofalo M, Romano G, Di Leva G, Nuovo G, Jeon YJ, Ngankeu A, et al. EGFR and MET receptor tyrosine kinase-altered microRNA expression induces tumorigenesis and gefitinib resistance in lung cancers. Nature medicine 2012;18(1):74-82.

39. Garofalo M, Di Leva G, Romano G, Nuovo G, Suh SS, Ngankeu A, et al. miR-221&222 regulate TRAIL resistance and enhance tumorigenicity through PTEN and TIMP3 downregulation. Cancer cell 2009;16(6):498-509.

40. Mudduluru G, Ceppi P, Kumarswamy R, Scagliotti GV, Papotti M, Allgayer H. Regulation of Axl receptor tyrosine kinase expression by miR-34a and miR-199a/b in solid cancer. Oncogene 2011;30(25):2888-99.

41. Lize M, Klimke A, Dobbelstein M. MicroRNA-449 in cell fate determination. Cell cycle 2011;10(17):2874-82.

42. Toyokawa G, Inamasu E, Shimamatsu S, Yoshida T, Nosaki K, Hirai F, et al. Identification of a Novel ALK G1123S Mutation in a Patient with ALK-rearranged Non-small-cell Lung Cancer Exhibiting Resistance to Ceritinib. Journal of thoracic oncology : official publication of the International Association for the Study of Lung Cancer 2015;10(7):e55-7.

43. Peng F, Xiong L, Tang H, Peng C, Chen J. Regulation of epithelial-mesenchymal transition through microRNAs: clinical and biological significance of microRNAs in breast cancer. Tumour biology : the journal of the International Society for Oncodevelopmental Biology and Medicine 2016.

44. Zang H, Wang W, Fan S. The role of microRNAs in resistance to targeted treatments of non-small cell lung cancer. Cancer chemotherapy and pharmacology 2016.

45. Svoronos AA, Engelman DM, Slack FJ. OncomiR or Tumor Suppressor? The Duplicity of MicroRNAs in Cancer. Cancer research

2016;76(13):3666-70.

46. Gao HX, Yan L, Li C, Zhao LM, Liu W. miR-200c regulates crizotinib-resistant ALK-positive lung cancer cells by reversing epithelial-mesenchymal transition via targeting ZEB1. Molecular medicine reports 2016.

47. Easwaran H, Tsai HC, Baylin SB. Cancer epigenetics: tumor heterogeneity, plasticity of stem-like states, and drug resistance. Molecular cell 2014;54(5):716-27.

48. Misso G, Di Martino MT, De Rosa G, Farooqi AA, Lombardi A, Campani V, et al. Mir-34: a new weapon against cancer? Molecular therapy Nucleic acids 2014;3:e194.

49. Richardson PG, Laubach JP, Lonial S, Moreau P, Yoon SS, Hungria VT, et al. Panobinostat: a novel pan-deacetylase inhibitor for the treatment of relapsed or relapsed and refractory multiple myeloma. Expert Rev Anticancer Ther 2015;15(7):737-48.

50. Wolf JL, Siegel D, Goldschmidt H, Hazell K, Bourquelot PM, Bengoudifa BR, et al. Phase II trial of the pan-deacetylase inhibitor panobinostat as a single agent in advanced relapsed/refractory multiple myeloma. Leukemia & lymphoma 2012;53(9):1820-3.

APPENDICES

Appendix 1. Phospho-receptor tyrosine kinase array showing increased phosphorylation of EGFR, HER2, HER3 and AXL in H3122 LR and H2228 LR cells, compared with parental cells.

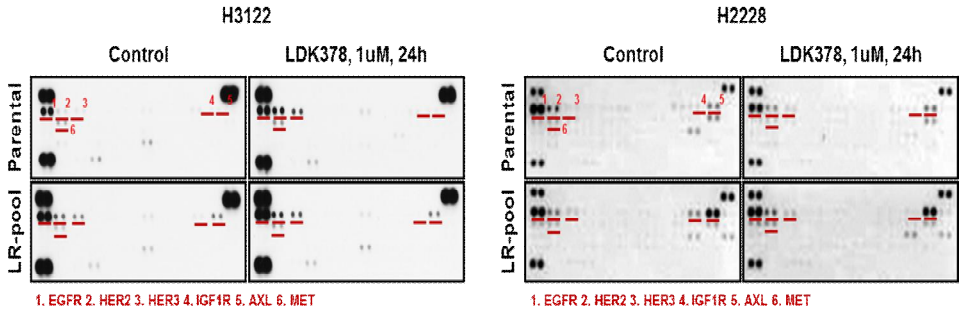

Appendix 2. Effects of mimics and inhibitors of miR-34a and miR-449 in H3122 LR and H3122 parental cells.

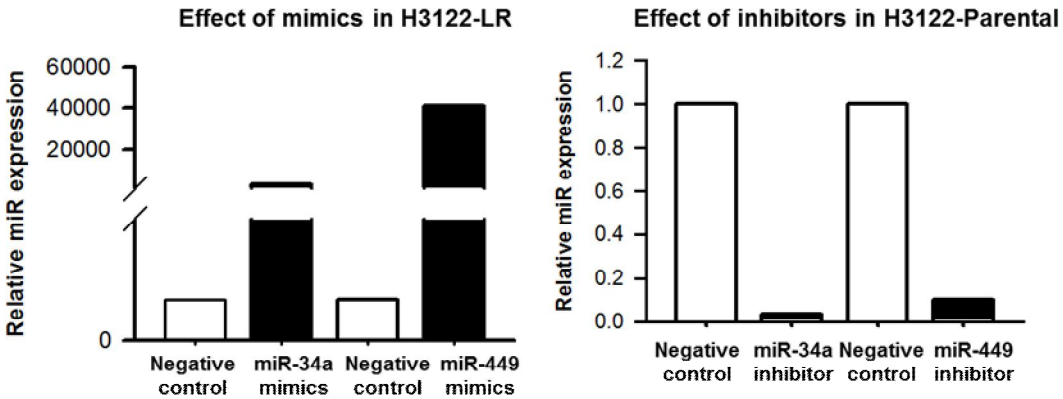

ABSTRACT(IN KOREAN)

miRNA-34a 와 miRNA-449a 의 후생유전학적 변화로 인한 epithelial-mesenchymal transition과 세리티닙에 대한 획득 내성 기전 규명

<지도교수 조 병 철>

연세대학교 대학원 의학과

임 선 민

EML4-ALK 양성 비소세포폐암 환자에서 ALK 타이로신 키나아제 억제제 치료 시 초기에는 우수한 반응을 보이나, 결국 약제 내성을 획득하게 된다. 비록 ALK 억제제에 대한 획득 내성 연구들이 진행된 바 있지만, 현재까지 후성유전학적 기전에 대한 연구는 전무하다. 본 연구에서는 세리티닙이라는 2세대 ALK 억제제에 대한 획득 기전 규명을 위해 RNA-seq, MBD-seq, ChIP-seq 통합 분석을 통해 내성 획득 세포의 전사체, DNA 메틸화, 히스톤 아세틸화 등 후성 유전체 통합 분석을 실행하였다. ALK 양성 내성 세포주에서 모세포주에 비해 H3K27ac 부위에 탈 아세틸화가 두드러지게 나타나는 것을 확인하였고, AXL 발현 증가와 상피-간엽전환 (epithelial-to-mesenchymal transition)이 발생하는 것을 확인하였다. H3K27 아세틸화 감소와 함께 mRNA 발현이 감소하는 유전자들을 선별한 결과, miR-34a와 miR-449a의 H3K27 탈아세틸화로 인하여 miR-34a와

miR-449a의 발현이 감소하고, 이에 따라 이들이 하위로 조절하는 AXL 과 mesenchymal 유전자들의 발현이 증가하는 기전을 규명하였다. 또한 AXL을 억제하거나 miR-34a 와 miR-449a를 외부에서 주입시켜 주었을 때 세리티닙에 대해 다시 민감성을 획득하였다. 히스톤 탈 아세틸화 효소 억제제인 Panobinostat에 의한 miR-34a 와 miR-449a의 탈 아세틸화 및 발현 조절이 가능한지 확인하기 위해 Panobinostat 처리 후 q-PCR, RNA-seq, ChIP-seq 분석을 수행하였고, Panobinostat 이 내성 세포주의 H3K27ac 부위에서 아세틸화를 증가시키는 것을 볼 수 있었다. Panobinostat을 세리티닙과 함께 내성세포주에 처리하였을 경우 병용효과를 확인할 수 있었고, G1 arrest 유도 단백질로 알려진 CDK inhibitor protein(CIP/KIP family)인 p21의 발현과, 세포사멸 (Apoptosis) 관련 단백질인 cleaved PARP와 cleaved caspase 3의 발현을 증가시킨 것을 확인하였다. 또한 miR-34a 및 miR-449 가 표적으로 하는 AXL 및 MET 등의 단백질 및 N-cadherin의 발현은 감소시켰고, 감소된 E-cadherin의 발현을 다시 증가시켰다. 상기 결과들을 통해 H3K27ac 리모델링으로 인한 miR-34a와 miR-449a 발현 감소가 세리티닙의 획득 내성에 중요한 역할을 하며, 이를 극복하기 위한 새로운 치료방법으로서 히스톤 탈 아세틸화 효소 억제제와 세리티닙의 병용 요법에 대한 전략을 제시해준다.

핵심되는 말: 비소세포폐암, 획득 내성, 세리티닙, 후성유전학